Scaled electron ionization cross sections in the Born approximation*

E. J. McGuire
Sandia Laboratories, Albuquerque, New Mexico 87115
(Received 25 February 1977)

The results of extensive calculations on cross sections for electron ionization of atomic subshells are presented in a scaled form. In general, the scaling is nonclassical, i.e., does not vary inversely with the square of the ionization potential. Comparison is made of the scaled $2p$ ionization cross section with measurements on Ar and Au, and good agreement is found. Comparison is made with measurements on cross sections for electron ionization of positive ions. The conclusion reached is that for ions with outer shells of low ionization potential, the scaled atomic cross sections are inaccurate, and that for such ions the cross sections are better described by the classical scaling law.

I. INTRODUCTION

It is well known that the cross section for K-shell ionization by electrons[1] and protons[2] satisfies a simple scaling law for all elements, in the nonrelativistic limit. The cross section (σ_{1s}) multiplied by the square of the $1s$-shell ionization energy is a function of projectile (electron or proton) energy divided by $1s$-shell ionization energy, i.e., $\sigma_{1s}(E_{1s})^2 = f(\epsilon/E_{1s})$. The plane-wave Born approximation (PWBA) predicts this scaling, as do other approximations; but while the PWBA agrees with measurements at $\eta_{1s} = \epsilon/E_{1s} > 4$, it overestimates $f(\epsilon/E_{1s})$ at small η_{1s}. As a practical matter, one can correct the PWBA scaled cross section with the measurements at low η. The question then arises, does this simplification occur for other subshells? Peart and Dolder[3] have shown that classical scaling does not hold for the $2p$ subshell by comparing the measured Ne $2p$ cross section with those of Na^+ and Mg^{+2}. However, I have elsewhere[4] reported calculations showing that for the $2p$ subshell of Ne to Ar, a nonclassical scaling law does hold, i.e., $\sigma_{2p}(E_{2p})^\alpha = g(\epsilon/E_{2p})$, where $\alpha \neq 2$. Vrakking and Meyer[5] have measured peak cross sections for the $2p$ subshell of Si, P, S, and Cl and find nonclassical scaling with an α close to the calculated one.

There are many areas of physics where scaled ionization cross sections are important, e.g., quantitative Auger surface spectroscopy,[1] the modeling of impurity effects in tokomak plasmas,[6] and the modeling of laser-produced plasmas.[7] In a nonhydrogenic treatment, even the PWBA is time-consuming on fast computers. But if reasonably simple scaling laws were valid, one could establish the scaling laws via a limited number of PWBA calculations. This is the approach followed here. As a minimum aim this paper presents, via scaling laws, a large body of computer calculations on atomic subshell cross sections. The cross sections are based on extensive calculations on the subshells of He to Ar, and a sampling of subshells and elements from K to Xe. Comparisons of these neutral-atom calculations with measured total cross sections are presented elsewhere.[8,9] Validation of the scaling laws is attempted via comparison with a limited amount of measurements on inner-shell electron ionization cross sections, and an extensive amount of data on electron ionization of positive ions.[10] In several instances, the comparison of measured positive-ion cross sections with those obtained from the scaled cross sections shows significant disagreement. At present it is not clear whether this arises from the use of the PWBA when the Coulomb-Born approximation is required, or that the scaling laws obtained from PWBA neutral-atom calculations do not reproduce PWBA calculations for the ions. PWBA calculations for a limited number of ions are currently being started.

The scaling laws are obtained by plotting $\sigma_{nl}(\max) \times (E_{nl})^2$ against E_{nl}. In classical scaling, this is a horizontal line. The choice of $\sigma_{nl}(\max)$ is somewhat arbitrary as σ_{nl} is obtained at a finite number of energy points. However, PWBA electron ionization cross sections have sufficiently broad maxima that little error should be introduced.

No attempt will be made in this paper to examine the origin of the scaling laws. At high η, the electron ionization cross section is related to photoionization cross section of the subshell. Scaling of the electron ionization cross section implies scaling of the photoionization cross section. This will be discussed in a later paper.

II. $2s$ AND $2p$ SUBSHELLS

In Fig. 1 is plotted the calculated peak electron ionization cross section multiplied by ionization energy squared versus ionization energy for the

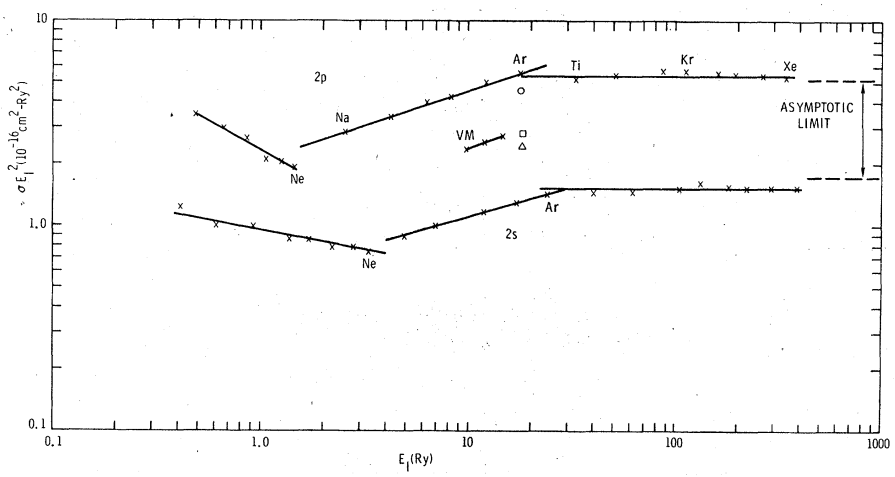

FIG. 1. Calculated $\sigma(\max)(E_I)^2$ for $2s$ and $2p$ subshells. The short line labelled VM is from Ref. 5, while the triangle, square, and circle are from Refs. 11, 12, and 13, respectively. The asymptotic limits are from $\sigma_{1s}(E_{1s})^2$.

$2s$ and $2p$ subshells. The energy is in rydbergs. For partially filled shells the calculated cross section is multiplied by an appropriate factor so that they become equivalent full-shell cross sections (for clarity the cross sections are presented for full shells, rather than per electron). The dashed curve labeled VM is the peak cross section of Vrakking and Meyer,[5] the triangle and square are the peak cross sections for the $2p$ subshell of Ar, as measured by Ogurtsov[11] and Christofzik,[12] respectively, and the circle is the Ar measurement of Langenberg *et al.*[13] The cross sections of Vrakking and Meyer, Ogurtsov, and Christofzik are based on the L_{23}-MM Auger yield. Langenberg *et al.* point out that this measures the total cross section in the absence of configuration interaction. Configuration interaction will result in Auger decay other than the L_{23}-MM transitions. Langenberg *et al.* correct their data for this effect and present a resultant total $2p$ ionization cross section. Assuming these considerations apply as well to the data of Vrakking and Meyer, and that the $2p$-subshell configuration-interaction mixing parameter is roughly constant from Si to Ar, there is then confirmation of the calculations in Fig. 1 over a limited range of ionization energy. From Fig. 1, it is clear that classical scaling is applicable for the $2s$ and $2p$ subshells at ionization energies greater than those for Ar. On the far right of Fig. 1, we show the scaled $1s$ values, i.e., $\sigma_{1s}E_{1s}^2$ and $3\sigma_{1s}E_{1s}^2$. That is, if there were no differences in shape, the classically scaled $1s$ cross section per electron would be identical with the classically scaled $2s$ and $2p$ cross sections per electron to better than 20%. From Fig. 1, it is clear that the cross sections can be divided into three regions: low energy with $\alpha > 2$, intermediate energy with $\alpha < 2$, and the region of classical scaling. In Table I are listed the energy bounds on the different regions, the appropriate values of α, and $f(\eta)$ vs η where $\eta = \epsilon/E_I$, where $f(\eta)$ is given per filled shell, and in units of 10^{-16} cm^2 R_y^α. The $f(\eta)$ values were obtained by suitably scaling a representative element. For the scaled $2p$ cross section in the region of classical scaling, I use the

TABLE I. Parameters for the scaled $2s$ and $2p$ electron ionization cross sections; $\sigma_{nl}(E_{nl})^\alpha = f_i(\epsilon/E_I)$, with f in units of 10^{-16} cm^2 R_y^α. The subscripts a, b, c refer to the following values for E and α:

$2s$	$2p$
a: $0.4 \leq E \leq 3.5$, $\alpha = 2.19$	a: $0.5 \leq E \leq 1.5$, $\alpha = 2.59$
b: $3.5 \leq E \leq 25.0$, $\alpha = 1.70$	b: $1.5 \leq E \leq 18$, $\alpha = 1.655$
c: $E \geq 25.0$, $\alpha = 2.00$	c: $E \geq 18$, $\alpha = 2.00$.

$2s$				$2p$			
η	f_a	f_b	f_c	η	f_a	f_b	f_c
1.25	0.130	0.115	0.31	1.25	0.23	0.30	1.05
1.5	0.265	0.245	0.75	1.5	0.54	0.66	2.20
1.75	0.380	0.340	1.10	1.75	0.82	1.00	3.20
2.0	0.480	0.425	1.30	2.0	1.06	1.27	4.05
2.5	0.645	0.510	1.50	2.5	1.46	1.66	4.95
3.0	0.770	0.535	1.60	3.0	1.76	1.86	5.40
3.5	0.880	0.545	1.60	3.5	1.98	1.96	5.60
4.0	0.930	0.540	1.58	4.0	2.15	2.00	5.70
5.0	0.930	0.510	1.50	5.0	2.32	1.99	5.50
6.0	0.900	0.480	1.40	6.0	2.40	1.91	5.20
7.0	0.860	0.445	1.30	7.0	2.40	1.83	4.86
8.0	0.800	0.415	1.22	8.0	2.38	1.75	4.60
10.0	0.700	0.360	1.07	10.0	2.27	1.60	4.10
15.0	0.535	0.272	0.80	15.0	1.96	1.25	3.20
20.0	0.435	0.222	0.65	20.0	1.69	1.04	2.60
25.0	0.372	0.188	0.550	25.0	1.48	0.89	2.20
30.0	0.322	0.164	0.475	30.0	1.30	0.78	1.90
40.0	0.258	0.130	0.375	40.0	1.07	0.63	1.52
50.0	0.215	0.108	0.310	50.0	0.91	0.525	1.28
60.0	0.185	0.094	0.267	60.0	0.80	0.425	1.10
80.0	0.145	0.073	0.210	80.0	0.64	0.355	0.87
100.0	0.120	0.060	0.174	100.0	0.54	0.300	0.74

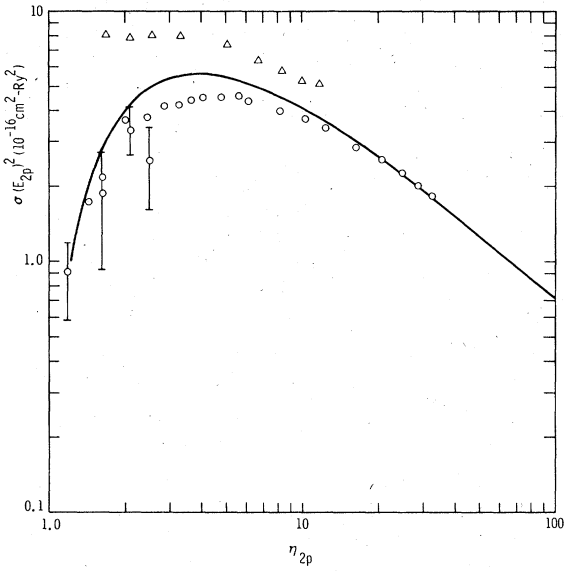

FIG. 2. Scaled $2p$ cross section in the classical region. The circles, points with error bars, and triangles are from Refs. 13, 15, and 16, respectively.

calculated Kr $2p$ cross section. In Fig. 2, I show the scaled Kr cross section as a solid line. The open circles are the Ar total-cross-section measurements of Langenberg *et al.*, scaled with the measured ionization energy,[14] 246 eV. Also shown, with error bars, are the L_2 and L_3 subshell measurements of Salem and Moreland[15] on Au, adjusted to a full shell (i.e., $3\sigma_{L_2}$, $1.5\sigma_{L_3}$). Finally the measurements of Davis *et al.*[16] on the L_3 subshell of Au are shown as triangles. There is a significant difference between the two sets of measured values for Au. However, the good agreement between the calculation and the data at $Z=18$ and $Z=79$, is substantial evidence that classical scaling is valid.

Next, the scaling laws are examined at low ionization energy. In Fig. 3, the calculated electron ionization cross sections obtained from Table I for Ne^+, Na^+, and Mg^{+2} are compared with the measurements of Dolder *et al.*,[17] Peart and Dolder,[3] and Peart *et al.*,[18] respectively. Also shown are the calculated $2s$-subshell cross sections. The calculated cross sections via Table I are in excellent agreement (20%) with the measurements, even though no account is taken of the charged nature of the interaction via the Coulomb-Born approximation. Moores[19] has done Coulomb-Born calculations on these three ions. At the peak, the cross sections of Moores are considerably higher than the measurements (>20%), with improved agreement at high energy. In Fig. 4 the calculated cross sections obtained from Table I (solid lines) for O, O^+, O^{+2} are compared with the measurements of Rothe *et al.*,[20] and Aitken and Harrison,[21] respectively. Agreement for O is excellent, but not surprising, as the direct calculation of the cross section was reported in Ref. 5, and the scaled cross sections are based on the direct calculation. For O^+ and O^{+2}, the calculation is lower than the measurements by a factor of 1.6. This is approxi-

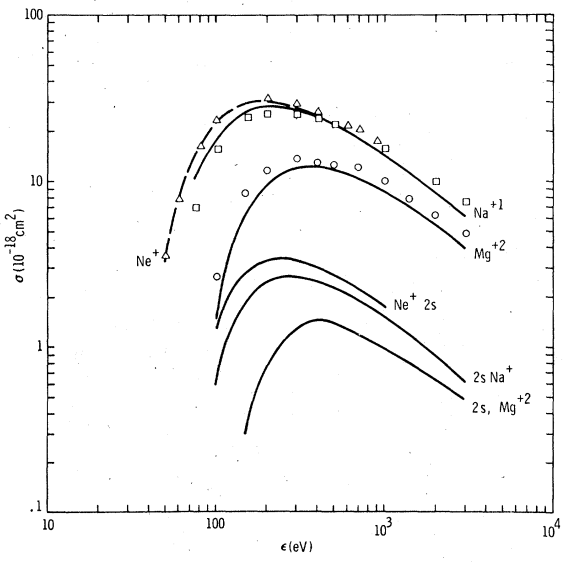

FIG. 3. Cross sections for electron ionization of Ne^+, Na^+, and Mg^{+2}. The triangles (Ne^+), squares (Na^+), and circles (Mg^{+2}) are from Refs. 17, 3, and 18, respectively.

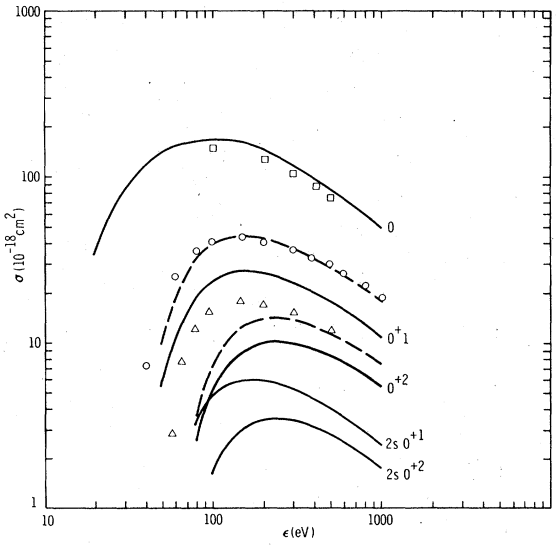

FIG. 4. Cross sections (solid curves) for electron ionization of O, O^+, and O^{+2}. The squares (O), circles (O^+), and triangles (O^{+2}) are from Ref. 20 and 21, respectively. The dashed curves are discussed in the text.

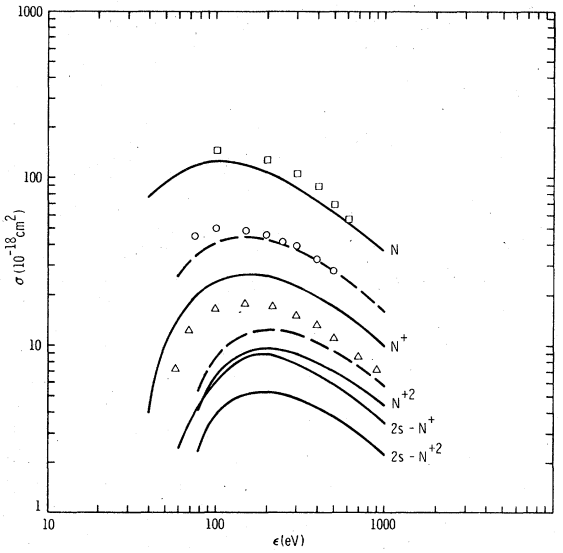

FIG. 5. Cross sections (solid curves) for electron ionization of N, N^+, and N^{+2}. The squares (N), circles (N^+), and triangles (N^{+2}) are from Refs. 22, 23, and 24, respectively. The dashed curves are discussed in the text.

mately the ratio of the classical $\sigma_{max}(E_I)^2$ to the actual $\sigma_{max}(E_I)^2$ in Fig. 1 at E_{2p} for the oxygen ions. When the calculated $2p$ cross section from Table I is corrected by this ratio, the results shown as dashed lines in Fig. 4 are obtained. This suggests that for the outer shell of ions with low E_I the classically scaled cross section is appropriate. However this would destroy the agreement for Ne^+, Na^+, and Mg^{+2}. It does suggest the hypothesis (which has not been checked) that PWBA calculations should be done for isoelectronic sequences of ions with outer shells of low E_I, that is, that for such isoelectronic sequences the approach to the classical scaling region is not along the neutral-atom curve in Fig. 1. In Fig. 5 the calculated cross sections obtained from Table I for N, N^+, and N^{+2}, are compared with the measurements of Smith *et al.*,[22] Harrison *et al.*,[23] and Aitken *et al.*,[24] respectively. The results and the discussion are almost identical to the case of oxygen ions. The Coulomb-Born calculations of Moores[19] are in excellent agreement with the measurements on oxygen and nitrogen ions.

III. $3s$, $3p$, AND $3d$ SUBSHELLS

In Fig. 6, $\sigma(\max)E_I^2$ is plotted against E_I for the $3s$, $3p$, and $3d$ subshells, as in Fig. 1. The $3d$ results are the open circles. There is some indication that classical scaling begins at Xe. The open triangles are the data of Vrakking and Meyer[5] for the $3d$ subshell of Br and Sn. The low values obtained by Vrakking and Meyer may result from neglect of configuration-interaction effects in detection via Auger yield measurements. The scaled cross sections are listed in Table II. For the $3d$ subshell only, do we list a cross section in the classical region. For the $3s$ and $3p$ subshells, Fig. 5 does not strongly indicate a classical region. However, if one wanted to extrapolate these cross sections to higher E_I via classical scaling, we have $\sigma(\mathrm{Xe}) = (E_{Xe})^{-\alpha} f_c(\epsilon/E_{Xe}) = (E_{Xe})^{-2} f_{ext}(\epsilon/E_{Xe})$, or for the classical region $\sigma(E_I)^2 = (E_{Xe})^{2-\alpha} f_c(\epsilon/E_{Xe})$, where E_{Xe} is the Xe $3s$ or $3p$ ionization potential

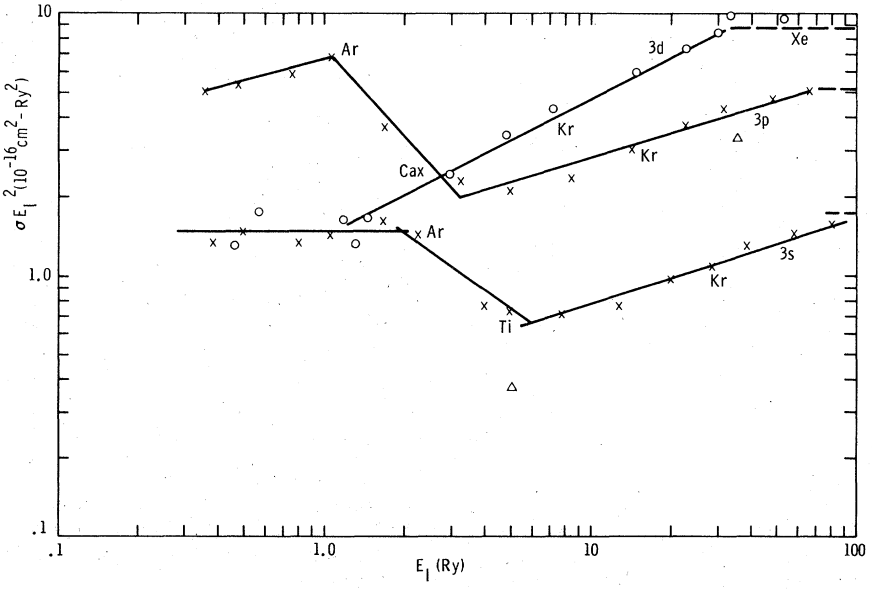

FIG. 6. Calculated $\sigma(\max)(E_I)^2$ for the $3s$, $3p$, and $3d$ subshells. The circles are the $3d$ values. The triangles are taken from Ref. 5.

TABLE II. Parameters for the scaled $3s$, $3p$, and $3d$ electron ionization cross sections; $\sigma_{nl}(E_{nl})^{\alpha}=f_i(\epsilon/E_I)$, with f in units of 10^{-16} cm^2 R_y^{α}. The subscripts a,b,c refer to the following values for E and α:

$3s$	$3p$	$3d$
a: $0.3\leq E\leq 2.0$, $\alpha=2.00$	a: $0.35\leq E\leq 1.1$, $\alpha=1.73$	a: $0.4\leq E\leq 1.1$, $\alpha=2.00$
b: $2.0\leq E\leq 6.0$, $\alpha=2.72$	b: $1.1\leq E\leq 3.2$, $\alpha=3.10$	b: $1.1\leq E\leq 35$, $\alpha=1.48$
c: $6.0\leq E\leq 80$, $\alpha=1.67$	c: $3.2\leq E\leq 66.0$, $\alpha=1.69$	c: $E\geq 35$, $\alpha=2.00$.

$3s$				$3p$				$3d$			
η	f_a	f_b	f_c	η	f_a	f_b	f_c	η	f_a	f_b	f_c
1.25	0.60	0.60	0.045	1.25	1.00	1.25	0.115	1.25	0.215	0.115	1.20
1.5	1.05	1.15	0.107	1.5	2.90	2.65	0.305	1.5	0.420	0.280	3.10
1.75	1.32	1.45	0.170	1.75	4.25	3.70	0.510	1.75	0.600	0.430	4.60
2.0	1.48	1.66	0.225	2.0	5.30	4.50	0.690	2.0	0.76	0.580	5.80
2.5	1.50	1.97	0.300	2.5	6.40	5.55	0.980	2.5	0.99	0.850	7.30
3.0	1.45	2.15	0.340	3.0	6.65	6.10	1.15	3.0	1.14	1.05	8.20
3.5	1.36	2.50	0.360	3.5	6.65	6.40	1.26	3.5	1.28	1.22	8.80
4.0	1.28	2.62	0.360	4.0	6.60	6.60	1.32	4.0	1.35	1.35	9.20
5.0	1.14	2.55	0.350	5.0	6.18	6.60	1.35	5.0	1.43	1.50	9.60
6.0	1.02	2.38	0.330	6.0	5.95	6.38	1.32	6.0	1.50	1.58	9.50
7.0	0.93	2.15	0.315	7.0	5.35	6.00	1.27	7.0	1.52	1.58	9.10
8.0	0.85	1.95	0.295	8.0	5.00	5.65	1.22	8.0	1.52	1.52	8.70
10.0	0.72	1.72	0.260	10.0	4.45	5.05	1.09	10.0	1.51	1.48	7.80
15.0	0.515	1.32	0.198	15.0	3.48	3.90	0.84	15.0	1.43	1.25	6.25
20.0	0.405	1.06	0.160	20.0	2.82	3.18	0.69	20.0	1.30	1.07	5.20
25.0	0.335	0.90	0.135	25.0	2.40	2.67	0.58	25.0	1.18	0.94	4.45
30.0	0.282	0.77	0.116	30.0	2.10	2.30	0.51	30.0	1.08	0.84	3.85
40.0	0.217	0.61	0.092	40.0	1.67	1.80	0.405	40.0	0.91	0.68	3.10
50.0	0.178	0.51	0.076	50.0	1.40	1.48	0.340	50.0	0.80	0.58	2.65
60.0	0.150	0.435	0.066	60.0	1.22	1.27	0.290	60.0	0.71	0.51	2.30
80.0	0.116	0.342	0.052	80.0	0.96	0.99	0.227	80.0	0.57	0.41	1.82
100.0	0.095	0.285	0.044	100.0	0.81	0.83	0.187	100.0	0.49	0.35	1.52
								200.0	0.29	0.20	0.89

and $f_c(\eta)$ is the scaled cross section in the highest energy range in Table II. There is no inner-shell data with which we can compare the results in Table II. There are two relevant elements for which positive-ion results exist. In Fig. 7, the cross sections calculated via Table II for Mg^+ and K^+ are compared with data of Martin *et al.*[25] and Peart and Dolder,[3] respectively. For Mg^+, the calculations are in excellent agreement with experiment. This agreement supports the suggestion that the measured atomic Na[8] and Mg[9] cross sections are probably in error. For K^+, the calculation via Table II (the solid line in Fig. 7) is lower than the data by a factor 1.6. As with the ions of oxygen and nitrogen, rescaling the Kr^+ $3p$ cross section to the classical value brings the calculated value (dashed line) in Fig. 7 into excellent agreement with the measurements.

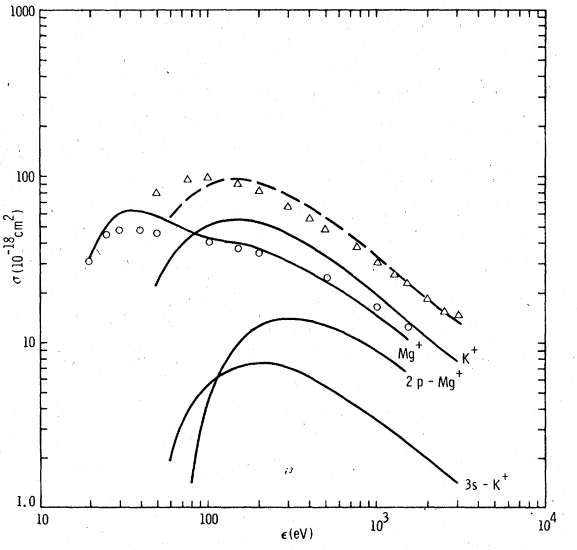

FIG. 7. Cross sections (solid lines) for electron ionization of Mg^+ and K^+. The circles (Mg^+) and triangles (K^+) are from Refs. 25 and 3, respectively. The dashed curve is discussed in the text.

IV. $4s$, $4p$, AND $4d$ SUBSHELLS

In Fig. 8, $\sigma(\max)E_I^2$ is plotted against E_I for the $4s$, $4p$, $4d$, and $5s$ subshells. The calculations cover a limited range of E_I; so little can be said

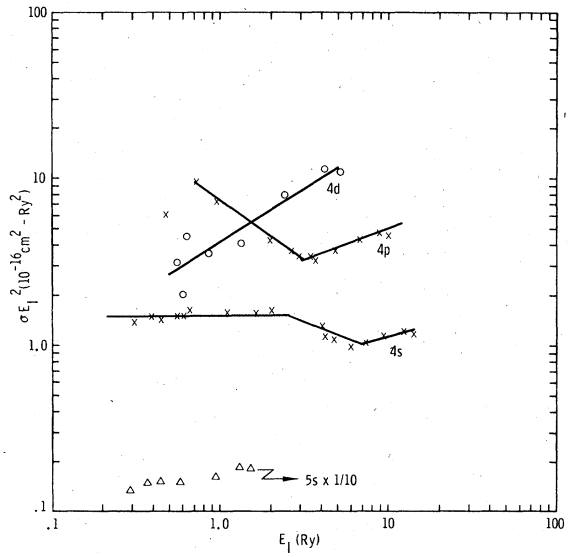

FIG. 8. Calculated $\sigma(\max)(E_I)^2$ for the $4s$, $4p$, $4d$, and $5s$ subshells. The $4d$ values are shown as circles, and the $5s$ values reduced by a factor of 10 are shown as triangles.

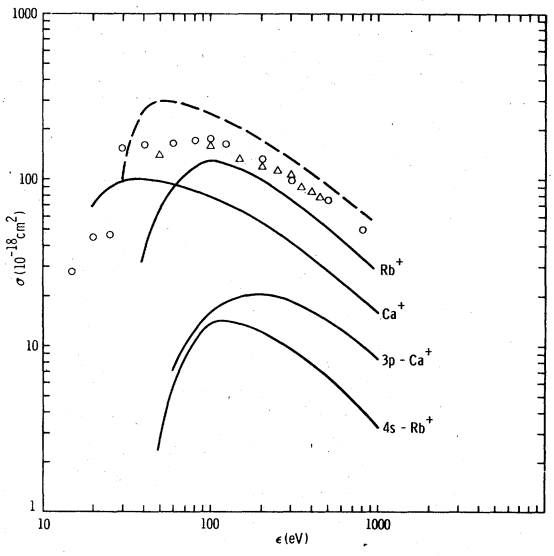

FIG. 9. Cross section (solid lines for electron ionization of Ca^+ and Rb^+). The circles (Ca^+) and triangles (Rb^+) are from Ref. 26. The dashed curve for Ca^+ includes inner-shell excitation followed by autoionization.

concerning the approach to the region of classical scaling. The scaled cross sections for the $4s$ and $4p$ subshells are listed in Table III. Again no inner-shell data exists, but there are data on electron ionization of positive ions. In Fig. 9, the cross sections calculated via Table III for Ca^+ and Rb^+ are compared with the data of Peart and Dolder.[26] For Rb^+ the cross section calculated via Table III agrees with the measurements to 25%. For Rb^+, correcting the calculated cross section to the classical limit introduces a factor of 1.17, improving the already good agreement. For Ca^+, the calculation is considerably below the measurements. Peart and Dolder[26] suggest that there may be considerable autoionization, i.e., $(3p)^6(4s) \rightarrow (3p)^5(4s)(3d)$ excitation followed by decay by electron emission. To check this suggestion, a calculation of the $(3p)^6 \rightarrow (3p)^5(3d)$ electron excitation cross section was performed. The potential used was for Ca^+ $(3p)^5(4s)^2$, used elsewhere to calculate Auger transition rates. When autoionization is included, the calculated effective electron ionization cross section for Ca^+ is given by the dashed curve in Fig. 9. My conclusion is that autoionization so masks the measurement in Ca^+ that no quantitative comparison can be made with the scaled cross section.

V. CONCLUSIONS

The results of a large number of calculations on the ionization of atomic subshells by electrons in the PWBA have been presented in scaled form.

TABLE III. Parameters for the scaled $4s$ and $4p$ electron ionization cross sections; $\sigma_{nl}(E_{nl})^\alpha = f_i(\epsilon/E_I)$, with f in units of 10^{-16} cm^2 R_y^α. The subscripts a, b, c refer to the following values for E and α:

$4s$	$4p$
a: $0.3 \leq E \leq 2.5$, $\alpha = 2.00$	a: $0.7 \leq E \leq 3$, $\alpha = 2.70$
b: $2.5 \leq E \leq 7.0$, $\alpha = 2.35$	b: $3 \leq E \leq 10$, $\alpha = 1.62$
c: $7 \leq E \leq 14$, $\alpha = 1.65$	

$4s$				$4p$		
η	f_a	f_b	f_c	η	f_a	f_b
1.25	0.50	0.60	0.11	1.25	1.05	0.24
1.5	0.84	1.15	0.30	1.5	2.45	0.72
1.75	1.13	1.60	0.44	1.75	3.70	1.20
2.0	1.32	1.92	0.46	2.0	4.80	1.65
2.5	1.50	2.12	0.48	2.5	6.40	2.10
3.0	1.52	2.15	0.47	3.0	7.30	2.10
3.5	1.50	2.10	0.46	3.5	7.45	2.05
4.0	1.44	2.00	0.44	4.0	7.40	1.97
5.0	1.32	1.78	0.42	5.0	7.00	1.82
6.0	1.20	1.58	0.38	6.0	6.50	1.67
7.0	1.10	1.40	0.35	7.0	6.00	1.55
8.0	0.98	1.28	0.32	8.0	5.50	1.42
10.0	0.82	1.08	0.28	10.0	4.75	1.23
15.0	0.58	0.76	0.215	15.0	3.50	0.91
20.0	0.45	0.59	0.172	20.0	2.75	0.71
25.0	0.36	0.48	0.145	25.0	2.30	0.58
30.0	0.30	0.40	0.124	30.0	1.95	0.50
40.0	0.225	0.30	0.097	40.0	1.50	0.385
50.0	0.185	0.245	0.080	50.0	1.23	0.320
60.0	0.155	0.190	0.068	60.0	1.05	0.270
80.0	0.115	0.155	0.053	80.0	0.80	0.217
100.0	0.093	0.125	0.043	100.0	0.67	0.175

Over a wide range of subshells and ionization energies the calculated scaled cross sections are nonclassical. That is, while one can represent the calculations via $\sigma_{nl}(E_{nl})^{\alpha}=f(\epsilon/E_{nl})$, α is not equal to 2 unless E_{nl} is sufficiently large. There is experimental evidence[3,5] that if scaling exists, it cannot be purely classical. Comparison of the scaled $2p$ cross section with available measurements on inner-shell electron ionization showed good agreement. There exists an extensive literature[2] on inner-shell proton ionization which will be treated in a later paper. Most of the comparisons of the scaled cross sections with experiment were with measurements of electron ionization of positive ions. In general, these measurements were in agreement with either the scaled cross section or with the scaled cross section adjusted to the classical scaled value. However, no criterion was found to distinguish the two cases. It is suggested that PWBA calculations on positive ions can illuminate the question of the approach to classical scaling along an isoelectronic sequence. I hope to do such calculations in the near future.

---

*Work supported by the United States Energy Research and Development Administration.

[1]C. J. Powell, Rev. Mod. Phys. 48, 33 (1976).
[2]J. D. Garcia, R. J. Fortner, and T. M. Kavanagh, Rev. Mod. Phys. 45, 111 (1973).
[3]B. Peart and K. T. Dolder, J. Phys. B 2, 240 (1968).
[4]E. J. McGuire, J. Phys. (Paris), Colloq. 10, 32, C4-37 (1971).
[5]J. J. Vrakking and F. Meyer, Phys. Rev. A 9, 1932 (1974).
[6]E. Hinnov, Phys. Rev. A 14, 1533 (1976).
[7]R. K. Landshoff and J. D. Perez, Phys. Rev. A 13, 1619 (1976).
[8]E. J. McGuire, Phys. Rev. A 3, 267 (1971).
[9]E. J. McGuire, preceding paper, Phys. Rev. A 16, 62 (1977).
[10]K. T. Dolder and B. Peart, Rep. Prog. Phys. 39, 693 (1976).
[11]G. N. Ogurtsov, Zh. Eksp. Teor. Fiz. 64, 1149 (1973) [Sov. Phys.-JETP 37, 584 (1973)].
[12]H. J. Christofzik, Diplom-thesis (University of Munster, 1970) (unpublished).
[13]A. Langenberg, F. J. deHeer, and J. van Eck, J. Phys. B 8, 2079 (1975).
[14]K. Siegbahn *et al.*, *ESCA, Atomic, Molecular and Solid State Structure Studied by Means of Electron Spectroscopy* (Almquist and Wiksells Boktryckeri AB, Uppsala, Sweden, 1967).
[15]S. I. Salem and L. D. Moreland, Phys. Lett. 37A, 161 (1971).
[16]D. V. Davis, V. D. Mistry, and C. A. Quarles, Phys. Lett. 38A, 169 (1972).
[17]K. T. Dolder, M. F. A. Harrison, and P. C. Thonemann, Proc. R. Soc. Lond. A 274, 546 (1963).
[18]B. Peart, S. O. Martin, and K. T. Dolder, J. Phys. B 2, 1176 (1969).
[19]D. L. Moores, J. Phys. B 5, 286 (1972).
[20]E. W. Rothe, L. L. Marino, R. N. Neynaber, and S. M. Trujillo, Phys. Rev. 125, 582 (1962).
[21]K. L. Aitken and M. F. A. Harrison, J. Phys. B 4, 1176 (1971).
[22]A. C. H. Smith, E. Caplinger, R. H. Neynaber, E. W. Rothe, and S. M. Trujillo, Phys. Rev. 127, 1647 (1962).
[23]M. F. A. Harrison, K. T. Dolder, and P. C. Thonemann, Proc. Phys. Soc. Lond. 82, 368 (1963).
[24]K. L. Aitken, M. F. A. Harrison, and R. D. Rundle, J. Phys. B 4, 1189 (1971).
[25]S. O. Martin, B. Peart, and K. T. Dolder, J. Phys. B 2, 537 (1968).
[26]B. Peart and K. Dolder, J. Phys. B 8, 56 (1975).